A general onepot-method for nucleic acid detection with CRISPR-Cas12a

Tang Guanghui (✉ tangguanghui@yanengbio.com)
Yaneng Biotech, Co., Ltd, Fosun Pharma, Shenzhen 518100 https://orcid.org/0000-0003-4585-9161

Jiaojiao Gong
Yaneng Biotech, Co., Ltd, Fosun Pharma, Shenzhen 518100

Lijuan Kan
Department of Laboratory Medicine, Luohu District People's Hospital, Shenzhen 518001

Xiuming Zhang
Department of Laboratory Medicine, Luohu District People's Hospital, Shenzhen 518001

Ying He
Department of Laboratory Medicine, the Eighth Affiliated Hospital, Sun Yat-sen University, Shenzhen 518033

Jiaqiang Pan
Yaneng Biotech, Co., Ltd, Fosun Pharma, Shenzhen 518100

Liping Zhao
Department of Laboratory Medicine, Nanning First People's Hospital, Nanning 530022

Jie Tian
Yaneng Biotech, Co., Ltd, Fosun Pharma, Shenzhen 518100

Sili Lin
Yaneng Biotech, Co., Ltd, Fosun Pharma, Shenzhen 518100

Zhouyu Lu
Yaneng Biotech, Co., Ltd, Fosun Pharma, Shenzhen 518100

Liang Xue
Yaneng Biotech, Co., Ltd, Fosun Pharma, Shenzhen 518100

Chaojun Wang
Department of Urology, the First Affiliated Hospital, Zhejiang University School of Medicine, Hangzhou 310003

Qianyun Li
Department of Neurology, Hwa Mei Hospital, University of Chinese Academy of Sciences, Ningbo 315010

Article

Keywords: CRISPR-Cas12a, nucleic acid detection, onepot reaction

Posted Date: July 24th, 2020

DOI: https://doi.org/10.21203/rs.3.rs-44613/v1

Abstract

CRISPR/Cas12a system has been shown promising for nucleic acid diagnostics due to its rapid, portable and accurate features. In combination with isothermal amplification technology, single-copy sensitivity can be achieved. However, cleavage of the amplicons and primers by the cis- and trans-activity of Cas12a hinders the attempts to integrate the amplification and detection steps into a single reaction.

Through phosphorothioate modification of primer and design of crRNA that allow for the cutting site locating at the modified site of the primer, we realized onepot detection of SARS-CoV-2 with single-copy sensitivity. We also identified the activated Cas12a has a much higher affinity to C nucleotide-rich reporter than others. By applying such reporters, we significantly reduced the reaction time required for the lateral-flow readout. Furthermore, to improve the specificity of the strip-based assay, we created a novel reporter and, when combined with a customized strip, the unspecific signal could be completely eliminated. This established system termed Targeting DNA by Cas12a-based Eye Sight Testing in Onepot Reaction (TESTOR) was validated using clinical cervical samples for human papillomaviruses (HPVs) detection.

Our system represents a general approach to integrating the nucleic acid amplification and detection into a onepot reaction in CRISPR-Cas systems, highlighting its potential as a rapid, portable and accurate detection platform of nucleic acids.

Introduction

Recent outbreak of SARS-CoV-2 has highlighted the challenges of detecting viral infections, especially in areas where specialized equipment is not available[1–3]. Polymerase chain reaction (PCR) is the most commonly used method and has been considered as a “gold standard” for nucleic acid diagnosis due to high sensitivity and specificity[4–6]. However, the requirement of expensive equipment and well-trained personnel as well as long reaction times (normally more than 2 h) makes it unsuitable for point-of-care test (POCT) diagnostics. These limitations hinder its applications in many cases and whereby delay the prescription and administration of antiviral agents to patients. In contrast, serology tests are rapid and require minimal equipment but have lower sensitivity and specificity[7,8]. It may need several days to weeks following symptom onset for a patient to mount a detectable antibody response[9].

CRISPR-Cas systems are adaptive immune systems in archaea and bacteria[10,11]. Some Cas nucleases display strong collateral activities after binding to their specific cis targets, which has been fully evaluated for diagnostic use[12–14]. By combination with recombinase polymerase amplification (RPA), Cas12 and Cas13 has been shown to permit single molecule detection in reactions[13,15,16]. Although both of them are RNA-guided nucleases[16], CRISPR/Cas13a may be less promising because it uses single stranded RNA (ssRNA) as reporters, which could be false-positive-prone, as RNases are common and highly stable in the environment.

In the addition to the commonly used RPA method, LAMP (loop-mediated isothermal amplification) and PCR approaches has also been reported to facilitate the Cas12a-based nucleic acid detection[17,18]. However, all of these methods have to separate the amplification step from the detection step owing to the fact that cleavage of the amplicons and primers by cis- and trans-activities of Cas12a could prevent the chain reactions. The requirement of nucleic acid pre-amplification makes this system more time-consuming and manpower demanding as well as generation of aerosol that usually causes false positive.

We herein report an assay termed **T**argeting DNA by Cas12a-based **E**ye **S**ight **T**esting in **O**nepot **R**eaction (TESTOR) for rapid, ultrasensitive and specific detection of nucleic acids. The primers were modified with phosphorothioate at certain sites to prevent the degradation by activated Cas12a. The crRNAs were designed to allow the cleavage on amplicons occur at the modified sites, whereby the amplicon can be just nicked, enabling the chain reactions to continue. We also optimized the reporters and identified that activated Cas12a has the highest affinity to C nucleotide-rich reporters, which enables us to reduce the required time of reaction. Furthermore, we designed a novel reporter labeled with FAM, DIG and Biotin, and modified with phosphorothioate at the sites between DIG and Biotin. When combined with a strip that can capture DIG and Biotin at the control and test line, respectively, the unspecific signal at the test line was completely eliminated.

This Cas12-based onepot nucleic acid detection platform (TESTOR) holds the potential to address the key challenges for viral diagnostics and will undoubtedly have a better clinical potential.

Result

Development of Cas12a-based TESTOR detection system

Studies of Cas12a-based diagnostics previously applied a separate pre-amplification step prior to Cas12a-mediated detection[14,17-19], which inevitably complicates the procedures and brings about contaminations. To simplify the operations, we attempted to develop an assay in which the components of RPA and Cas12a enzyme were added all together in a single reaction. As an application example, we first designed primers and crRNA targeting N gene of severe acute respiratory syndrome coronavirus 2 (SARS-CoV-2), a novel coronavirus responsible for the COVID-19 global pandemic. After incubation of the RPA with Cas12a at 37 °C for 40 minutes, however, there was no signal detected (**Fig. 1a**).

Previous study showed that Cas12 family enzymes generate double-strand DNA breaks in a sequential dependent manner. The non-target DNA strand cleavage is known to precede target DNA strand cleavage. The cleavage of the NTS in dsDNA substrates activates the collateral activity of Cas12a and initiates cleavage of non-target substrates[20]. As the single-stranded primers could also be a substrate of the activated Cas12a, we hypothesized that both cleavage of the amplicons and degradation of the primers contribute to the failing detection of the target gene. To verify this, we performed phosphorothioate modifications at multiple sites of primers (**Fig. 1b**). Such modifications is typically resistant to the

cleavage by divalent cation-dependent nucleases[20,21]. A crRNA overlapping multiple nucleotides with the primer was designed, which enables the cleavage by Cas12a-crRNA complex occur at the modified sites[20]. As shown in **Fig. 1c**, the non-target strand without modifications would be cleaved while the target strand would keep intact after cleavage. Although the detailed mechanisms are unclear, this nicked structure might serve as a template for the DNA amplification, enabling continuously production of amplicons. When incubating the components of RPA and Cas12a in onepot at 37°C, RPA amplification is first initiated and the amplified target sequence is recognized by Cas12a-crRNA complex. The Cas12a endonuclease is then activated and cleaves the nearby FQ reporters to generate fluorescence (**Fig. 1d**).

In initial experiments with the modified primers, we were surprised to find a strong signal accumulation over time when target was present in the reaction (**Fig. 1e, S1a**). Nevertheless, when we tried to repeat this finding with other primer pairs, the signals become extremely weak (**Fig. S1b, S1c**), suggesting instability of this onepot system. To investigate either failed amplification of the nucleic acid or unsuccessful cleavage of the amplicons by Cas12a contributed to the faint signal, we resolved the reactions by agarose electrophoresis. Consistent with the fluorescent signals, three out of five reactions showed obvious bands whereas the rest two had little products (**Fig. S1d**). To identify whether the observed bands were the intended products, 5 mL of the reaction was added into 45 mL of 1X Cas12a mixture. Similar trends were observed but the signals were much stronger compared to that of the onepot assay (**Fig. S1d**). We wondered if the RPA reaction system might impede the collateral activity of activated Cas12a, because RPA reaction system is rather viscous. By adding additional 5 mL of water into the onepot system, we found a remarkable increase of signals generated by cleaved reporters (**Fig. S1e**). These observations drove us to think that if the inhibited cleavage of reporter was resulted from the evaporation of the reaction as an uncapped 96-well plate was used during the monitoring process. We therefore switched to a capped PCR detection system for signal monitoring. As expected, a strong fluorescence increasing was observed after incubation at 37^{o}C for 20 min (**Fig. 1f**).

We next evaluated the limit of detection (LoD) of the TESTOR system. Whereas our onepot assay lacked the sensitivity to detect single-copy molecule, it unambiguously identified 10 copies of target in the reaction within a relative longer time (approximate 1 hour; **Fig. 1g**). To assess whether this primer-modified method can serve as a general way for Cas12a-based onepot detection, we designed other primer sets targeting a different region of N (N2) and ORF1ab gene of SARS-CoV-2. In the presence of high number of targets, all reactions for both N2 and ORF1ab could readily distinguish their corresponding targets from NTC (non-target control) within a short incubation time (**Fig. 1h, S2a**). However, when copy numbers in the system were low, the fluorescence-differential time was bit long, and all cases failed to detect single-copy molecule (**Fig. 1i, S2b, S2c**). Together, these results reveal the feasibility of Cas12a-based onepot detection by phosphorothioate modifications on the backbone of primers.

Optimization of TESTOR assay

To achieve a better sensitivity in a shorter time, we first evaluated the effect of primer concentration on the efficiency of our assay. As shown in **Fig. 2a**, we found the optimal concentration was 0.32 μM. Cleavage efficiency of CRISPR/Cas9 systems seemed to be influenced by GC content and purine residues in the gRNA end[22]. We were therefore interested in knowing whether the trans activity of Cas12a was dependent on the sequence of reporters. We found that C nucleotide-rich reporters exhibited the strongest fluorescence signal, indicating the highest affinity of this reporter to crRNA-Cas12a complex (**Fig. 2b, S3a, S3c**). Interestingly, the G nucleotide reporter showed negligible increase of fluorescence, implying there was almost no cleavage induced by crRNA-Cas12a complex (**Fig. 2b**). We further tested the specificity of these reporters, and none of them showed obvious signal increasing over time in NTC groups (**Fig. S3b, s3c**). Besides, we found two sites of modification on the ends of forward and reverse primers is sufficient to trigger the strongest detection. However, too many modifications seemed to inhibit the reaction (**Fig. 2c**). We thus used a condition of two-site modified primers at the concentration of 0.32 μM for each and combined with C nucleotide-rich reporters in the reaction for the following experiments.

With these optimizations, we compared the canonical two-step method with TESTOR assay in the presence of 100 copies of target in the reaction. The former of which began to produce signal upon incubation at 37^{o}C, while the latter showed a lag around 10 minutes before reporter cleavage (**Fig. 2d-2f**). This phenomenon could be explained by the required time for amplicon accumulation before recognition and cleavage by crRNA-Cas12a complex. Moreover, we examined the analytic performance of this optimized system for detection of N gene and demonstrated it had a sensitivity of single-copy (**Fig. 2g**).

Development of a lateral flow TESTOR assay

For any on site detection assays, pairing with a visual readout is crucial especially in situations when instruments are not available. We herein developed a method enabling colorimetric readout with a lateral flow strip. We designed a reporter with a dye label (FAM) on the 5’ end and a biotin on the 3’ end. When coupled with a ready-to-use strip (**Fig. 3a**), the destruction of the reporter is visible by naked eye. As described previously[23], the control line captures abundant reporter that binds to anti-FAM antibody-gold conjugates with streptavidin molecules, which prevents accumulation of the antibody-gold conjugates to secondary antibodies on the test line; the cleaved reporter-antibody-gold conjugates flow over the control line and will be fixed there by species-specific antibodies on the test line (**Fig. 3a**).

Whereas the positive samples displayed an easy-to-see band after 5 min of lateral flow in the diluted reaction solution (1:5), a faint signal, in the absence of target, was also present at the test line (**Fig. 3b**). This unspecific signal was even more obvious when the dilution ratio increased from 1:5 to 1:10 (**Fig. 3c**). Time point monitoring demonstrated the unspecific band was produced as early as 1 min of incubation at room temperature (**Fig. 3c**).

In clinical applications, presence of an unspecific faint band at the test line would make judgement of positivity rather difficult, as weak positive samples can also give a faint signal. The unspecific band

might be generated by the antibody-gold conjugates that did not bind to intact or destroyed reporter, making it a problem rather tough to be solved[17]. Here, we designed a novel reporter labeled with biotin, FAM and DIG (**Fig. 3d**), and modified with phosphorothioate at the sites between DIG and Biotin. Besides, we created a dipstick on which the gold particles were coupled with the biotin-ligand molecules in the sample application area, and anti-FAM antibodies and anti-DIG antibodies were immobilized on the control and test line, respectively. When reacted solution with the novel reporter was applied onto the strip, intact reporter will be trapped by anti-FAM antibodies at the first line while the degraded reporter without FAM fluorophore on its 3' end will be captured by anti-DIG antibodies at the second line. As a proof-of-concept assay, we first tested our novel system using N gene of SARS-CoV-2 and demonstrated it was highly specific, and did not yield any signal at the test line in NTC group (**Fig. 3e, 3f**). Moreover, the signal was much stronger when the reporter was modified with phosphorothioate compared to that without such modification (**Fig. 3e**). The inhibited cleavage at the site between biotin and DIG, which leads to increased accumulation of intact ssDNA-antibody-gold conjugates at the test line, may contribute to this result. To confirm it, we applied a phsphorothioate modified reporter that was labeled with a FAM molecule on its 5' end and a BHQ1 quencher in the middle, and found the fluorescence produced by the reporter cleavage was completely abolished (**Fig. 3g, 3h**). Consistent with the results obtained by fluorescence, the C-nucleotide-rich reporter was able to shorten the reaction time in lateral flow assay as well (**Fig. 3i**). These results indicate that the TESTOR system for lateral flow assay is of high rapidity and specificity.

TESTOR validation with clinical samples for detection of HPV16 and HPV18

Human papillomaviruses (HPVs) are the major causative agents of cervical carcinomas with types 16 (HPV16) and 18 (HPV18) accounting for most precancerous lesion[24]. We designed sets of primers targeting L1 region of HPV16 or HPV18, and selected the best performance primer pairs for a rapid and sensitive detection (**Fig. S4**). We then used the selected primer pairs to test extracted DNA from 53 cervical scrape samples taken with a cytobrush. Of the 53 samples, 20 and 12 were positive for HPV16 and HPV18 infection, respectively, by qPCR testing, and 21 were negative for HPV16 or HPV18 infection but either positive for other type of HPVs or negative by all testing. All positive samples for HPV16 or HPV18 by qPCR were positive in our assay, confirming that the false negative rate for TESTOR is very low (**Fig. 4a-4d, S5**). However, 1 out of 20 the PCR-negative samples showed slight increase in fluorescence when the reaction time was more than 40 min (**Fig. S6**). To explore whether the signal was generated by specific activation of Cas12a, we performed PCR amplification using the product. The amplified solution was then subjected to Cas12a detection but, as shown in **Fig.4e**, no signal was detected, indicating the signal was generated by unspecific reporter cleavage, which may be due to the long incubation time. Together, our onepot TESTOR assay had 100% positive and negative agreements relative to the qPCR assay, for detection of the HPV16 and HPV18 in a total of 53 clinical samples.

Next, we evaluated our established lateral flow system using 20 positive and 20 negative cervical scrape samples. The positive and negative agreements of the TESTOR assay relative to the qPCR assay were 100%, for detection of both HPV16 and HPV18. One samples with HPV18 infection gave a very faint band at the test line, which is consistent with its qPCR result, revealing the advantages of our established lateral flow system over the traditional one in detecting samples with low viral load, as there was no unspecific signal at all at the test line in negative samples. These data together illustrate the high sensitivity and specificity of the TESTOR assay.

Discussion

In present study, we provide a general onepot method for Cas12a-based nucleic acid detection by modifying the primers with phosphorothioate and designing crRNA allowing the cleavage occur at the modified sites. With these innovations, we integrate the amplification and detection into a single reaction system, which is highly valuable as avoidance of uncapping is important for prevention of aerosol generation that easily causes false positivity. Previous studies adopted a physical separation method to combine nucleic acid amplification and Cas12a detection into a single tube[16,25]. Wang et. al. added Cas12a on the inner wall of the reaction tube, and a centrifugation step was followed to initiate the cis- and trans-cleavage of Cas12a after RPA reaction[16]. However, this method is troublesome and also unreliable. The TESTOR system applies all components into a single common-used tube, which completely circumvents the preamplification of target nucleic acids and the requirement of special tubes or devices[26]. We also report here, for the first time, that the trans activity of the activated Cas12a prefers a C-nucleotide sequence. By leveraging this feature, the reaction time for a sensitive detection was significantly reduced when C-nucleotide rich reporters were used. To make it more field deployable, we created a novel lateral flow assay, which surmounts the shortcoming of the routine lateral flow method, and provided a more specific strip-based system.

Our TESTOR system needs minimal instrumentation and can be performed by lay users, making it suitable for diagnostic tests in resource-restricted areas. As proof-of-concept assays, TESTOR has been developed for SARS-CoV-2 detection. The infection cases of SARS-CoV-2 are increasing rapidly around the world and it seems now to be driven by community transmission[27,28]. As numerous infections are asymptomatic, nucleic acid testing is vital to differentiate infected from healthy individuals[29]. Therefore, a rapid diagnostic method for SARS-CoV-2 is urgently needed. Our Cas12a-based TESTOR technology can be reconfigured within days to detect SARS-CoV-2 and has the promise to address the key challenges for this global pandemic. We also validated the TESTOR system using specimens for HPV detection. By combining with a rapid sample processing method, the sample-to-result can be achieved in 30 minutes with high sensitivity (1-10 copies per reaction, data not shown).

Our system reported here could be an alternative to qRT–PCR test as it is faster, simpler and highly specific.

To facilitate routine surveillance of pathogens and other comprehensive applications, integration of the TESTOR with microfluidic system would be necessary because in many cases there is a need for diagnostic technologies to be able to test many samples while simultaneously testing for many targets. A recent study developed a massive multiplexing system for nucleic acid detection by combining a microwell array that harnesses solution-based fluorescent color codes with CRISPR-Cas13 detection. This novel system is capable of testing >4,500 crRNA-target pairs on a single array[30]. Another appealing development in the future for TESTOR would be accommodation of a portable cartridge to streamline the workflow and to enable point-of-care testing in in diverse environments, such as airports, clinics, local communities and other locations. The cartridge could also reduce the risk of aerosol contamination as all processes including sample manipulation, onepot reaction and lateral flow strip visualization could be completed in a closed-evironment[31].

Methods

Nucleic acid preparation

The synthetic DNA fragment of ORF1ab or N gene was ligated into a pUC19 vector (BIOLIGO, Shanghai, China) and amplified in E.coli. system. Plasmid DNA was extracted with a commercially available kit (Tiangen, Wuxi, China) and the concentration was quantified using a spectrophotometer (Thermo Fisher, NJ, USA). Copy number of the plasmid was calculated based on the concentration using the following equation: DNA copy number = $(M \times 6.022 \times 10^{23})/(n \times 1x10^{9} \times 650)$, in which M represents the amount of DNA in nanograms, n is the length of the plasmid in base pair, and the average weight of a base pair is assumed to be 650 Daltons.

Primer selection

RPA primers for SARS-CoV-2 and HPVs detection were designed according to a protocol described by Twist-Dx (Maidenhead, UK). Primer pairs were screened using a single forward primer against all reverse primers, where the best reverse primer was selected and then used to screen all the forward primers. The best performance primer pairs were used in subsequent experiments.

Cas12a detection reactions

The RPA or PCR product (5 µL) was mixed with 20 µL of the Cas12a reaction mixture containing 50 nM Cas12a (NEB, Ipswich, UK), 100 nM crRNA (BIOLIGO, Shanghai, China), and 250 nM ssDNA reporter (Sangon, Shanghai, China). Then, signal was collected using a fluorescence plate reader (Molecular Devices, California, USA) or a Real-Time PCR Detection System (Bio-Rad, Watford, UK) for up to 120 minutes at 37°C.

Fluorescence TESTOR assay

Each lyophilized pellet from the Basic DNA RPA kit was resuspended in a solution comprising 29.4 mL of rehydration buffer, 4 mL of primer mix each at 5 mM, 10.1 mL of H_2O. This mix was then divided into 2 parts, with each comprising 21.75 mL, and followed by addition of 2 mL of template DNA, 1.25 mL magnesium acetate (280mM) and 6.25 mL of 5x Cas12a mixture containing NEB 2.1 reaction buffer, 250nM Cas12a enzyme, 500nM crRNA, and 1.25mM ssDNA reporters. Reactions were incubated in a Real-Time PCR Detection System for up to 120 minutes at 37°C with fluorescent signals collected every 30 s (ssDNA FQ reporter = lex: 485 nm; lem: 535 nm). For all endpoint analysis, fluorescence was taken at 30 min after reaction.

Lateral flow TESTOR assay

The components of strip-based TESTOR reaction was similar to that for fluorescence-based TESTOR assay, except replacing the FQ reporter with a ssDNA labelled with Biotin, DIG and FAM. The reaction was incubated at 37°C for 30 minutes, followed by dilution at the indicated ratio in Tris-HCL buffer (0.05M, PH=7.6), and then a strip (TwistDx, Cambridge, UK; Bioustar, Hangzhou, China) was inserted and incubated at room temperature. After 2 minutes of incubation, the strip were removed and photographed with a smartphone camera.

Specimen collection and DNA extraction for HPV detection

A conventional cytological scrape was taken with a cytobrush from women visiting the gynecological outpatient clinic of the Shenzhen Luohu People's Hospital in China. The specimens were placed into tubes containing 3 mL of cell collection medium (Yaneng Bio, Shenzhen, China) and stored at -20^{O}C until use. Total DNA was extracted by using a lysis buffer containing 800 mM guanidine hydrochloride, 50 mM Tris-HCl (pH 8.0), 1% Triton X-100, and 0.5% Tween-20. The pellets from 1mL of the liquid-based cervical cytology samples after centrifugation were mixed with 200mL of the lysis buffer and heated for 10 min at 95^{O}C. The supernatant was used for HPV detection assays following a centrifugation step.

qPCR assay for HPV testing

HPV DNA was detected using a HPV test kit (Yaneng Bio, Shenzhen, China) according to the instruction of manufacturer. The assay was performed using the Biorad CFX96 instrument, with the following program:

pre-denaturation at 95^{o}C for 10 minutes, denaturation at 95^{o}C for 10 seconds, and annealing and extension as well as signal detection at 55^{o}C for 45 seconds.

All the primers, crRNAs and reporters used in this study are listed in **Table 1**.

Declarations

Acknowledgements: We thank Wei He and Jing Qu for comments and discussion and Yuanyuan Chang for preparation of the HPV plasmids. This study was supported by the Shenzhen Key Medical Discipline Construction Fun.

Conflict of interest

The authors declare no competing financial interests.

References

1 Zhu, N. *et al.* A Novel Coronavirus from Patients with Pneumonia in China, 2019. *N Engl J Med* **382**, 727-733, doi:10.1056/NEJMoa2001017 (2020).

2 Wang, C., Horby, P. W., Hayden, F. G. & Gao, G. F. A novel coronavirus outbreak of global health concern. *Lancet* **395**, 470-473, doi:10.1016/S0140-6736(20)30185-9 (2020).

3 Rothe, C. *et al.* Transmission of 2019-nCoV Infection from an Asymptomatic Contact in Germany. *N Engl J Med* **382**, 970-971, doi:10.1056/NEJMc2001468 (2020).

4 Radmard, S. *et al.* Clinical Utilization of the FilmArray Meningitis/Encephalitis (ME) Multiplex Polymerase Chain Reaction (PCR) Assay. *Front Neurol* **10**, 281, doi:10.3389/fneur.2019.00281 (2019).

5 Wang, A. M., Doyle, M. V. & Mark, D. F. Quantitation of mRNA by the polymerase chain reaction. *Proc Natl Acad Sci U S A* **86**, 9717-9721, doi:10.1073/pnas.86.24.9717 (1989).

6 Ding, X., Yin, K., Li, Z. & Liu, C. J. b. All-in-One dual CRISPR-cas12a (AIOD-CRISPR) assay: a case for rapid, ultrasensitive and visual detection of novel coronavirus SARS-CoV-2 and HIV virus. (2020).

7 Bosch, I. *et al.* Rapid antigen tests for dengue virus serotypes and Zika virus in patient serum. *Sci Transl Med* **9**, doi:10.1126/scitranslmed.aan1589 (2017).

8 Balmaseda, A. *et al.* Antibody-based assay discriminates Zika virus infection from other flaviviruses. *Proc Natl Acad Sci U S A* **114**, 8384-8389, doi:10.1073/pnas.1704984114 (2017).

9 Zhang, W. *et al.* Molecular and serological investigation of 2019-nCoV infected patients: implication of multiple shedding routes. **9**, 386-389 (2020).

10 Barrangou, R. *et al.* CRISPR provides acquired resistance against viruses in prokaryotes. **315**, 1709-1712 (2007).

11 Marraffini, L. A. & Sontheimer, E. J. J. s. CRISPR interference limits horizontal gene transfer in staphylococci by targeting DNA. **322**, 1843-1845 (2008).

12 Gootenberg, J. S. *et al.* Multiplexed and portable nucleic acid detection platform with Cas13, Cas12a, and Csm6. **360**, 439-444 (2018).

13 Myhrvold, C. *et al.* Field-deployable viral diagnostics using CRISPR-Cas13. *Science* **360**, 444-448, doi:10.1126/science.aas8836 (2018).

14 Chen, J. S. *et al.* CRISPR-Cas12a target binding unleashes indiscriminate single-stranded DNase activity. *Science* **360**, 436-439, doi:10.1126/science.aar6245 (2018).

15 Zhang, F., Abudayyeh, O. O. & Gootenberg, J. S. J. A. p. f. d. o. C.-u. C. d. A protocol for detection of COVID-19 using CRISPR diagnostics. **8** (2020).

16 Wang, B. *et al.* Cas12aVDet: A CRISPR/Cas12a-Based Platform for Rapid and Visual Nucleic Acid Detection. *Anal Chem* **91**, 12156-12161, doi:10.1021/acs.analchem.9b01526 (2019).

17 Broughton, J. P. *et al.* CRISPR-Cas12-based detection of SARS-CoV-2. *Nat Biotechnol*, doi:10.1038/s41587-020-0513-4 (2020).

18 Li, S.-Y. *et al.* CRISPR-Cas12a has both cis-and trans-cleavage activities on single-stranded DNA. **28**, 491-493 (2018).

19 Li, S.-Y. *et al.* CRISPR-Cas12a-assisted nucleic acid detection. **4**, 1-4 (2018).

20 Swarts, D. C. & Jinek, M. J. M. c. Mechanistic Insights into the cis-and trans-Acting DNase Activities of Cas12a. **73**, 589-600. e584 (2019).

21 Eckstein, F. & Gish, G. Phosphorothioates in molecular biology. *Trends Biochem Sci* **14**, 97-100, doi:10.1016/0968-0004(89)90130-8 (1989).

22 Bruegmann, T., Deecke, K. & Fladung, M. Evaluating the Efficiency of gRNAs in CRISPR/Cas9 Mediated Genome Editing in Poplars. *Int J Mol Sci* **20**, doi:10.3390/ijms20153623 (2019).

23 Gootenberg, J. S. *et al.* Multiplexed and portable nucleic acid detection platform with Cas13, Cas12a, and Csm6. *Science* **360**, 439-444, doi:10.1126/science.aaq0179 (2018).

24 Zur Hausen, H. & De Villiers, E.-M. J. A. r. o. m. Human papillomaviruses. **48**, 427-447 (1994).

25 Wang, Y., Ke, Y., Liu, W., Sun, Y. & Ding, X. J. A. s. A one-pot toolbox based on Cas12a/crRNA enables rapid foodborne pathogen detection at attomolar level. **5**, 1427-1435 (2020).

26 Wu, H., He, J.-s., Zhang, F., Ping, J. & Wu, J. J. A. C. A. Contamination-free visual detection of CaMV35S promoter amplicon using CRISPR/Cas12a coupled with a designed reaction vessel: rapid, specific and sensitive. **1096**, 130-137 (2020).

27 Liu, J. *et al.* Community transmission of severe acute respiratory syndrome coronavirus 2, Shenzhen, China, 2020. (2020).

28 Ghinai, I. *et al.* Community transmission of SARS-CoV-2 at two family gatherings—Chicago, Illinois, February–March 2020. (2020).

29 Shaman, J. & Galanti, M. J. m. Direct Measurement of Rates of Asymptomatic Infection and Clinical Care-Seeking for Seasonal Coronavirus. (2020).

30 Ackerman, C. M. *et al.* Massively multiplexed nucleic acid detection with Cas13. 1-6 (2020).

31 Joung, J. *et al.* Point-of-care testing for COVID-19 using SHERLOCK diagnostics. (2020).

Table

Table 1. Primers, crRNAs and reporters used in this study

Oligo name	Oligo Sequence(5'-3')	Usage
STD-N-F1	CCAGGCAGCAGTAGGGGAACTTCTCCTGCTAGAAT	Fig. 1a
STD-N-F2	CAGGCAGCAGTAGGGGAACTTCTCCTGCTAGAAT	Fig. 1a
STD-N-F3	TCAACTCCAGGCAGCAGTAGGGGAACTTCTCC	Fig. 1a
STD-N-R1	GTTGGCCTTTACCAGACATTTTGCTCTCAAGCTGG	Fig. 1a
STD-N-R2	TGGCCTTTACCAGACATTTTGCTCTCAAGCTG	Fig. 1a
STD-N-R3	TTACCAGACATTTTGCTCTCAAGCTGGTTCAA	Fig. 1a
N-F0	G*G*AACTTCTCCTGCTAGAATGGCTGGCAAT*G*G	Fig. 1e, 1g; Fig. S1a; throughout the paper when N gene was examined unless otherwise stated
N-R0	G*G*CCTTTACCAGACATTTTGCTCTCAAGCT*G*G	Fig. 1e, 1g; Fig. S1a; throughout the paper when N gene was examined unless otherwise stated
N-F01	G*GAACTTCTCCTGCTAGAATGGCTGGCAATG*G	Fig. 2c
N-R01	G*GCCTTTACCAGACATTTTGCTCTCAAGCTG*G	Fig. 2c
N-F02	G*G*A*ACTTCTCCTGCTAGAATGGCTGGCAA*T*G*G	Fig. 2c
N-R02	G*G*C*CTTTACCAGACATTTTGCTCTCAAGC*T*G*G	Fig. 2c
N-F03	G*G*A*A*CTTCTCCTGCTAGAATGGCTGGCA*A*T*G*G	Fig. 2c
N-R03	G*G*C*C*TTTACCAGACATTTTGCTCTCAAG*C*T*G*G	Fig. 2c
N-F1	C*C*AGGCAGCAGTAGGGGAACTTCTCCTGCTAGA*A*T	Fig. S1b-S1e
N-F2	C*A*GGCAGCAGTAGGGGAACTTCTCCTGCTAGA*A*T	Fig. S1b-S1e
N-F3	T*C*AACTCCAGGCAGCAGTAGGGGAACTTCT*C*C	Fig. S1b-S1e
N-F4	A*G*AAATTCAACTCCAGGCAGCAGTAGGGGAA*C*T	Fig. S1b-S1e
N-F5	G*C*AGTAGGGGAACTTCTCCTGCTAGAATGG*C*T	Fig. 1f; Fig. S1b-S1e
N-F6	G*T*TCAAGAAATTCAACTCCAGGCAGCAGTA*G*G	Fig. 1f
N-R1	G*T*TGGCCTTTACCAGACATTTTGCTCTCAAGCT*G*G	Fig. 1f; Fig. S1b-S1e
N2-F	A*G*AGGCGGCAGTCAAGCCTCTTCTCGTTCCTC*A*T	Fig. 1h, 1i
N2-R	C*A*GGAGAAGTTCCCCTACTGCTGCCTGGAG*T*T	Fig. 1h, 1i
ORF1ab-F11	T*T*GCCTGGCACGATATTACGCACAACTAATG*G*T	Fig. S2a, S2b
ORF1ab-F18	A*T*GGTGACTTTTTGCATTTCTTACCTAGAGT*T*T	Fig. 2d-2f ; Fig. S2a, S2c
ORF1ab-R2	A*A*GTCAGTGTACTCTATAAGTTTTGATGGTGT*G*T	Fig. 2d-2f ; Fig. S2a-S2c
HPV16-F1	G*T*TACAACGAGCACAGGGCCACAATAAT*G*G	Fig. S4a, S4b
HPV16-F2	C*C*CAAATATTCAATAAACCTTATTGGTTACA*A*C	Fig. S4b
HPV16-F3	A*A*TATTCAATAAACCTTATTGGTTACAACGAGC*A*C	Fig. S4b
HPV16-F4	G*G*TTACAACGAGCACAGGGCCACAATAATGG*C*A	Fig. S4b; throughout the paper when HPV16 was examined unless otherwise stated
HPV16-R1	C*C*CATGTCGTAGGTACTCCTTAAAGTTAGTATT*T*T	Fig. S4a
HPV16-R2	A*C*TCCTTAAAGTTAGTATTTTTATATGTAG*T*T	Fig. S4a
HPV16-R3	T*A*CTGCGTGTAGTATCAACAACAGTAACAA*A*T	Fig. S4a, S4b; throughout the paper when HPV16 was examined unless otherwise stated
HPV16-R4	T*A*TTTGTACTGCGTGTAGTATCAACAACAG*T*A	Fig. S4a
HPV16-R5	T*A*GTATCAACAACAGTAACAAATAGTTGGT*T*A	Fig. S4a
HPV18-F1	G*C*ATAATCAATTATTTGTTACTGTGGTAGATACC*AC*T	Fig. S4c, S4d
HPV18-F2	A*T*AACAATGGTGTTTGCTGGCATAATCAATTAT*T*T	Fig. S4d
HPV18-F3	T*G*GTTACATAAGGCACAGGGTCATAACAAT*G*G	Fig. S4d
HPV18-F4	A*A*TTATTTGTTACTGTGGTAGATACCACTCGC*A*G	Fig. S4d; throughout the paper when HPV18 was examined unless otherwise stated
HPV18-F5	C*A*CAGGGTCATAACAATGGTGTTTGCTGGCAT*A*A	Fig. S4d
HPV18-R1	A*A*ATTTGGTAGCATCATATTGCCCAGGTAC*A*G	Fig. S4c, S4d

HPV18-R2	T*G*GTAGCATCATATTGCCCAGGTACAGGAGAC*T*G	Fig. S4c, S4d; throughout the paper when HPV18 was examined unless otherwise stated
HPV18-R3	T*A*GCATCATATTGCCCAGGTACAGGAGACTG*T*G	Fig. S4c
HPV18-R4	T*T*GGTAGCATCATATTGCCCAGGTACAGGAGAC*T*G	Fig. S4c
HPV18-R5	T*T*GGTAGCATCATATTGCCCAGGTACAGGAG*A*C	Fig. S4c
qPCR primers and probes	Proprietary	Fig. 4b, 4d; Fig. S5; Fig. S6; Fig. S7; Fig. S8;
crRNA-N	UAAUUUCUACUAAGUGUAGAUcugcugcuugacagauugaacc	throughout the paper when N gene was examined unless otherwise stated
crRNA-N2	UAAUUUCUACUAAGUGUAGAUuugaacuguugcgacuacgugau	Fig. 1h, 1i
crRNA-ORF1ab	UAAUUUCUACUAAGUGUAGAUgugcaguugguaacaucuguuac	Fig. 2d-2f; Fig. S2
crRNA-HPV16	UAAUUUCUACUAAGUGUAGAUuuggggguaaccaacuau	throughout the paper when HPV16 was examined
crRNA-HPV18	UAAUUUCUACUAAGUGUAGAUacaauaugugcuucuacaca	throughout the paper when HPV18 was examined
n-reporter-0	/56-FAM/TTATT/3Bio/	Fig. 3a-3c
FQ1	/56-FAM/TTATT/3BHQ1/	Fig. 1a, 1e-1i; Fig. 2a, 2c; Fig. S1; Fig. S2; Fig. S3; Fig. S4
FQ3	/56-FAM/TTCCTT/3BHQ1/	Fig. S3
FQ4	/56-FAM/TTCCCTT/3BHQ1/	Fig. S3
FQ5	/56-FAM/TTCCCCCTT/3BHQ1/	Fig. S3
FQ7	/56-FAM/TTCCCCTT/3BHQ1/	Fig. S3
FQ8	/56-FAM/AAAAAA/3BHQ1/	Fig. 2b
FQ9	/56-FAM/TTTTTT/3BHQ1/	Fig. 2b
FQ10	/56-FAM/GGGGGG/3BHQ1/	Fig. 2b
FQ11	/56-FAM/CCCCCC/3BHQ1/	Fig. 2b; Fig. 4; Fig. S3; Fig. S5; Fig. S6; Fig. S7; Fig. S8
reporter-1	/56-FAM/T(dT-BHQ1)ATT	Fig. 3h
reporter-2	/56-FAM/T*(dT-BHQ1)ATT	Fig. 3h
reporter-3	/56-FAM/T(dT-BHQ1)CCCCTT	Fig. 3i
reporter-4	/56-FAM/T*(dT-BHQ1)CCCCTT	Fig. 3i
n-reporter-1	/56-Bio/T(dT-DIG)ATT/3FAM/	Fig. 3e
n-reporter-2	/56-Bio/T*(dT-DIG)ATT/3FAM/	Fig. 3e, 3j
n-reporter-3	/56-Bio/T*(dT-DIG)CCCCTT/3FAM/	Fig. 3j; Fig. 5

Figures

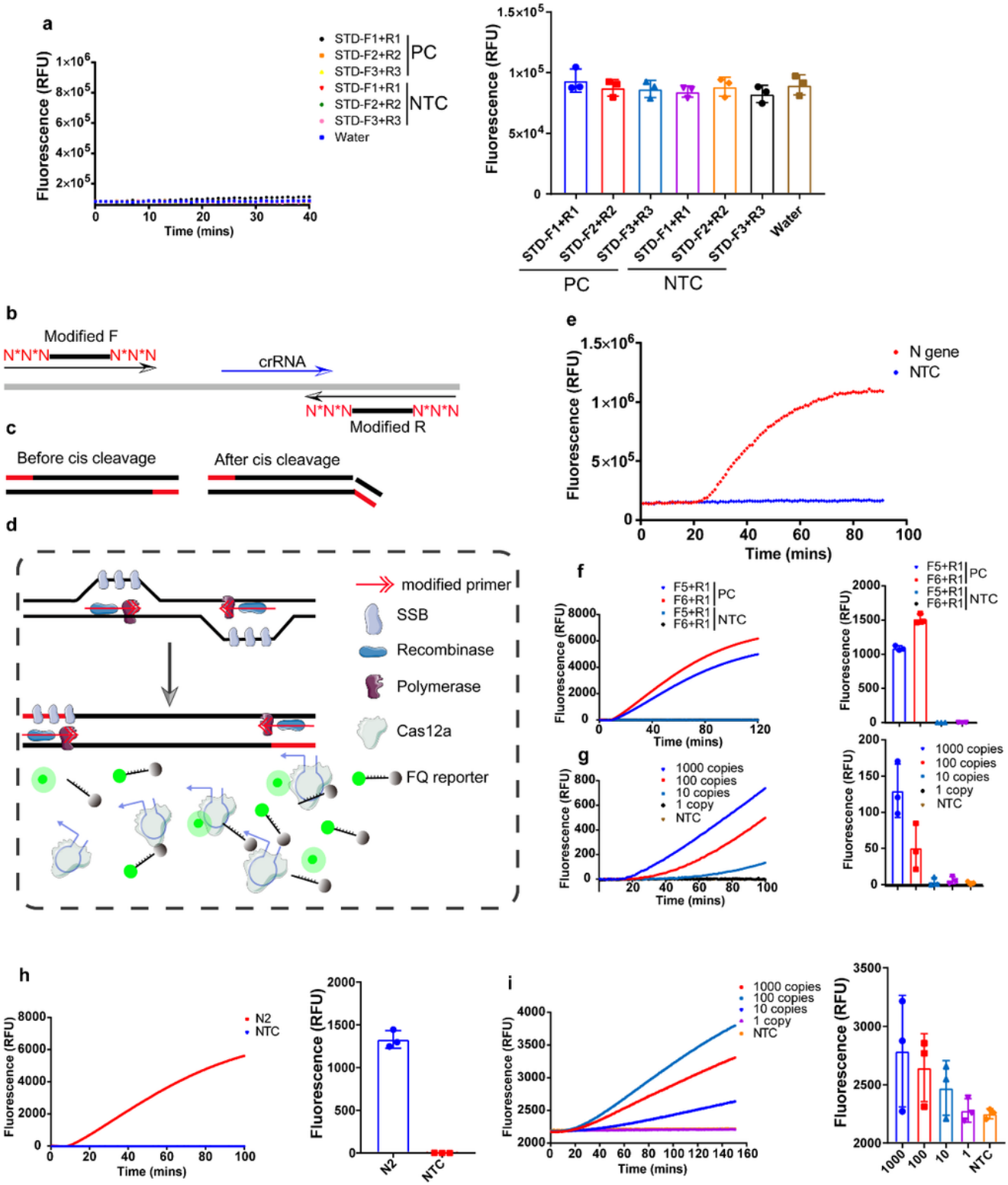

Figure 1

Detecting N gene of SARS-CoV-2 with a onepot method using phosphorothioate modified primers. a, Representative plot of fluorescence intensity versus time for onepot detection of N gene of SARS-CoV-2 using three unmodified-primer pairs (left panel). Fluorescent signal was obtained at 30 minutes after reaction (right panel). b, Primers were modified with phosphorothioate on the first two phosphate backbones proximity to 5' or 3' end. crRNA was designed to have two nucleotides overlapping with the

reverse primer (upper panel). Modified F: forward primer modified with phosphorothioate; modified R: reverse primer modified with phosphorothioate. c, Intact amplicons derived from the modified primers (left panel) and nicked dsDNA products after Cas12a cis cleavage (right panel). d, Schematic of TESTOR workflow. SSB, single-stranded DNA binding protein; F, fluorophore; Q, quencher. e, Real-time fluorescence detection of the TESTOR assay for N gene of SARS-CoV-2 and 105 copies of plasmid DNA was used. f, Fluorescence kinetics of two primer pairs for N gene of SARS-CoV-2 detection (left panel) in a closed-tube. Fluorescent signal was measured at 30 minutes after reaction (right panel) using 105 copies of plasmid DNA. g, Analytical sensitivity of TESTOR for N gene of SARS-CoV-2 detection (left panel). Fluorescent signal was measured at 30 minutes after reaction (right panel) using 105 copies of plasmid DNA. h, Another region of N gene of SARS-CoV-2 (N2) was detected using 105 copies of plasmid DNA template. i, Analytical sensitivity of TESTOR for N2 gene of SARS-CoV-2 detection. Signals were obtained using a plate reader in an uncapped 96-well plate (a, e) or using an real-time PCR detection system in a capped PCR tube (f, g, h, i). Error bars represent the mean ± s.d., where n = 3 replicates (a, f, g, h, i).

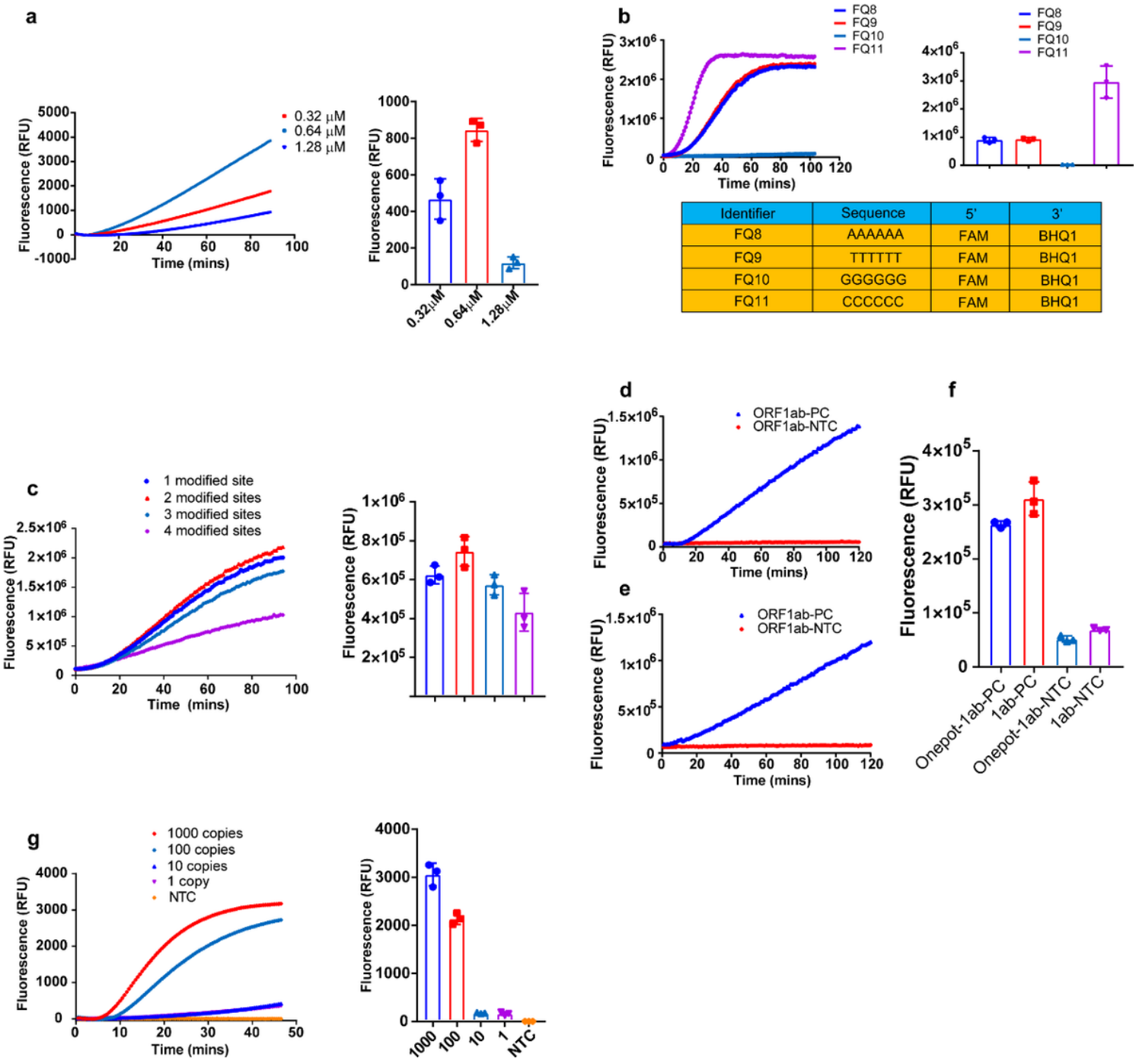

Identifier	Sequence	5'	3'
FQ8	AAAAAA	FAM	BHQ1
FQ9	TTTTTT	FAM	BHQ1
FQ10	GGGGGG	FAM	BHQ1
FQ11	CCCCCC	FAM	BHQ1

Figure 2

Optimization of TESTOR system. a, Real-time (left panel) and end point (right panel) fluorescence detection using primers specific to the N gene at the indicated concentration. b, Reporters with A, T, G, or C nucleotide sequence was screened to identify the one with the best affinity to Cas12a. The same amount of RPA product of N gene was added to a Cas12a mixture with different reporter, and fluorescence was monitored by real-time or taken at 30 min after incubation at 37oC. c, Primers modified with phosphorothioate on different phosphate backbones were compared for reaction efficiency by real-time (left panel) or endpoint (right panel) method. d, TESTOR approach for detection of ORF1ab gene of SARS-CoV-2. e, Fluorescence kinetics of Cas12a cleavage using product of RPA for ORF1ab gene as input. f,

Quantification of the fluorescence intensity of TESTOR method or routine two-step method (from fig. 2d and fig. 2e) after 30 minutes of incubation at 37oC. g, Determination of LoD for N gene using the optimized conditions for TESTOR system. Representative plot of fluorescence intensity over time for N gene of SARS-CoV-2 (left panel) or fluorescent signal was taken at 30 minutes after reaction (right panel). Error bars represent the mean ± s.d., where n = 3 replicates (b, e, f, g).

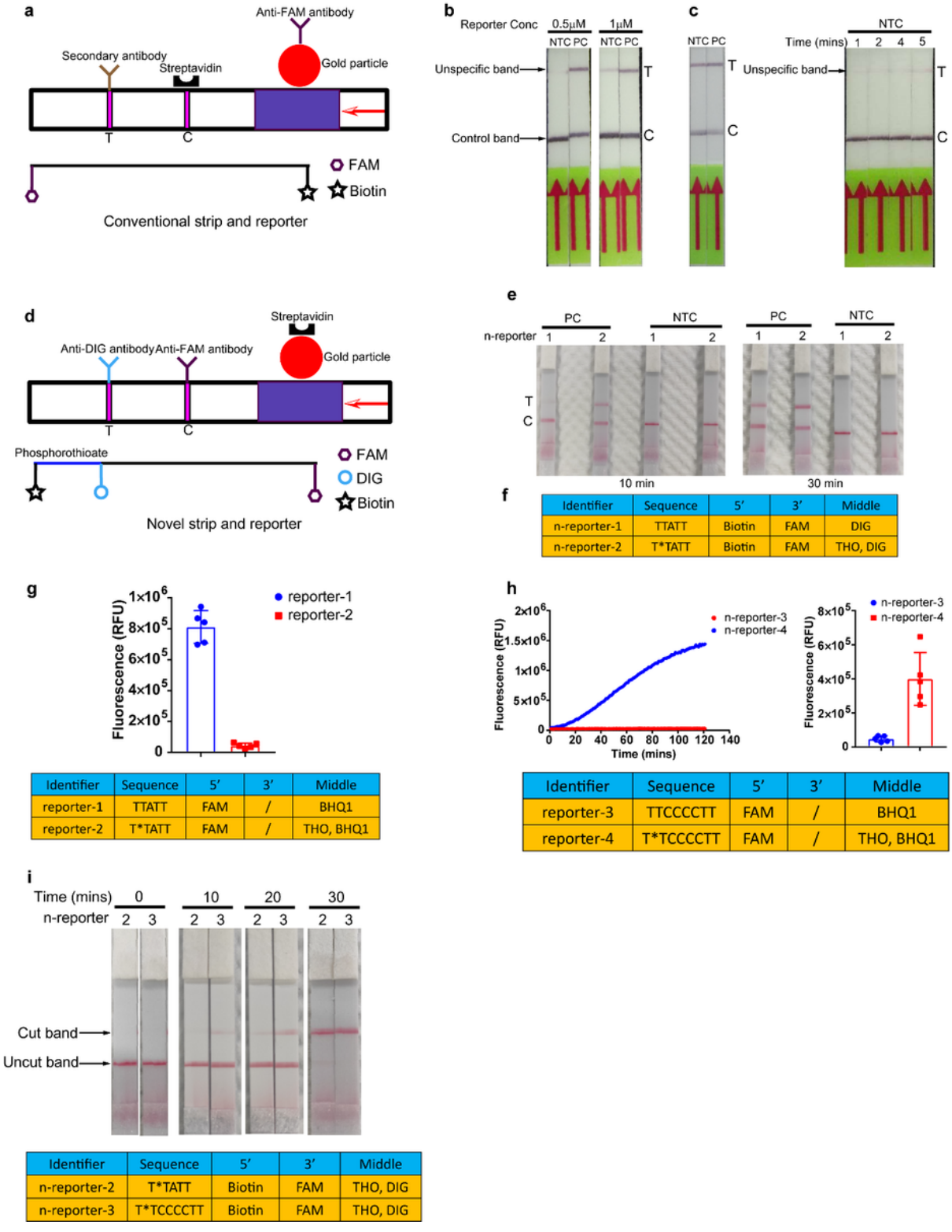

Figure 3

Development of novel lateral flow assay. a, Schematic of conventional strip and reporter used for Cas12a-based nucleic acid detection. b, Lateral flow strip readout of 1:5 diluted TESTOR reactions with 0.5□M or 1□M reporter in the presence or absence of N gene target using conventional strip and reporter. Strip was incubated at room temperature for 5 min following 30 min of TESTOR reaction at 37oC. c, Lateral flow strip readouts of 1:10 diluted TESTOR reactions with 1□M reporter in the presence or absence of N gene target using conventional strip and reporter (left panel). Time course of lateral flow strip readouts using 1:5 diluted TESTOR reactions with 1□M reporter in the absence of N gene target (right panel). d, Schematic of the novel strip and reporter. The reporter is labeled with a biotin on 5’ end, a FAM molecule on its 3’ end and a DIG in the middle. Anti-FAM and Anti-DIG antibodies are immobilized at the control and test line, respectively. e, Lateral flow strip readouts using novel strip and reporter at indicated conditions. Novel reporters with or without the phosphorothioate modification between biotin and DIG were used to perform the lateral flow assay. f, Sequences of novel reporters; * and THO represent phosphorothioate modification. g, Fluorescence obtained at 30 min after reaction using two different reporters with or without phosphorothioate modification (upper panel). Sequences and modification of reporters; * and THO represent phosphorothioate modification (bottom panel). h, Representative plot of fluorescence intensity versus time (upper left) and its quantification (upper right) after 30 min of reaction using C nucleotide-rich reporters. Sequences and modification of reporters; * and THO represent phosphorothioate modification (bottom panel). i, Comparison of cleavage efficiency for C nucleotide-rich and –lacking reporters at specified conditions (upper panel). Sequences and modification of reporters; * and THO represents phosphorothioate modification (bottom panel).

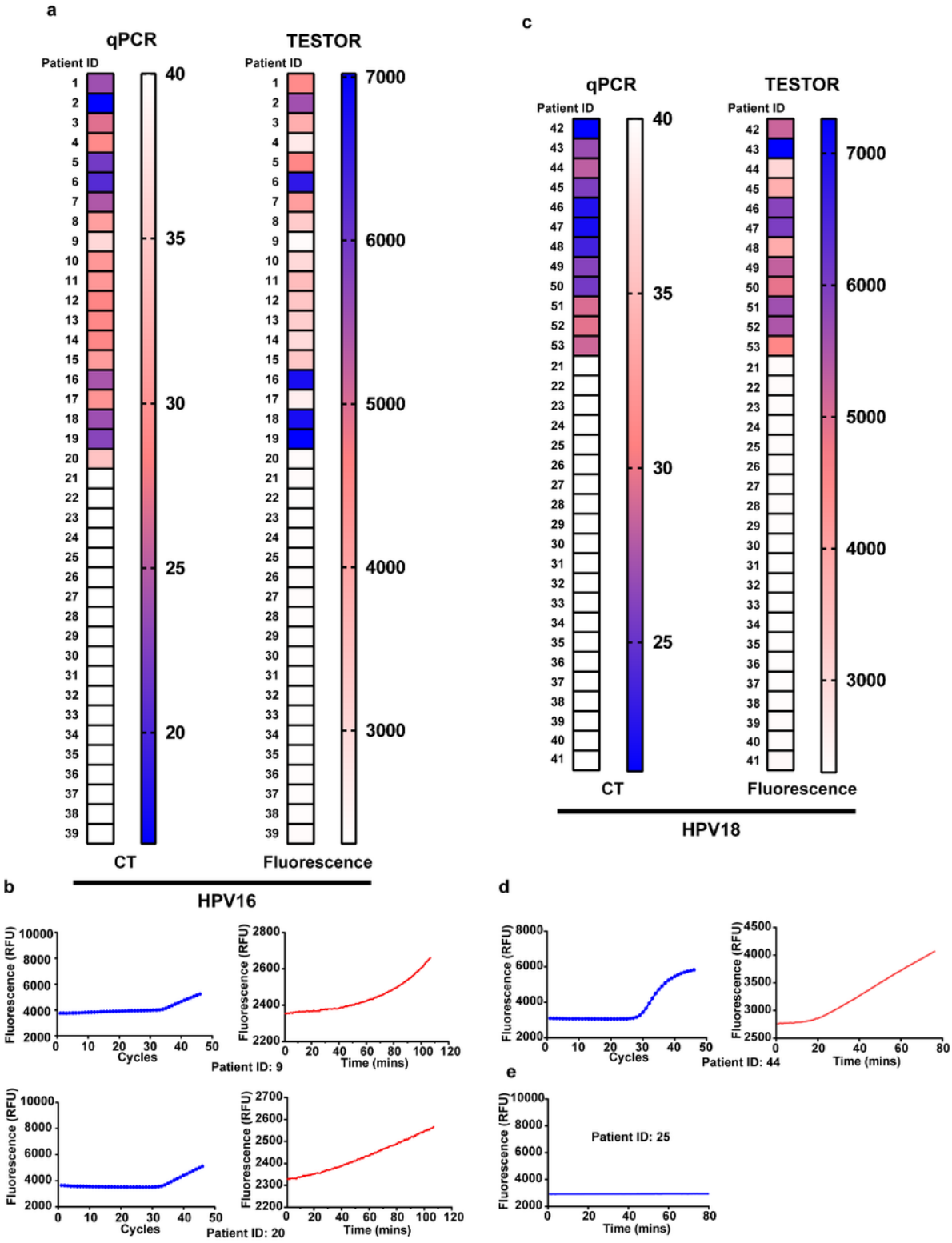

Figure 4

Detection of HPV in clinical samples using fluorescence TESTOR assay. a, Heatmaps showing the CT values by qPCR (left panel) and fluorescence at 30 min by TESTOR assay (right panel) for HPV16 detection. Two out of twenty clinical samples were qPCR positive but showed weak signal at 30 minutes by TESTER assay (Patient ID: 9, 20). b, Fluorescence kinetics of the two samples showing late CT values by qPCR or weak signals by TESTER. c, Results of the qPCR (left panel) and fluorescence TESTOR assay

at 30 min (right panel) for HPV18 detection. One out of thirteen clinical samples was positive by qPCR but showed weak signal at 30 minutes by fluorescence TESTER assay (Patient ID: 44). d, Fluorescence kinetics of the clinical sample (Patient ID: 44) showing late CT value by qPCR or weak signal by TESTOR assay. e, Fluorescence curve of re-examination by Cas12a for one patient negative for HPV18 by qPCR but showing slight signal increase by TESTOR. The yield of TESTOR from the patient (ID: 25) was amplified by PCR and then the PCR product was detected by Cas12a reaction.

a

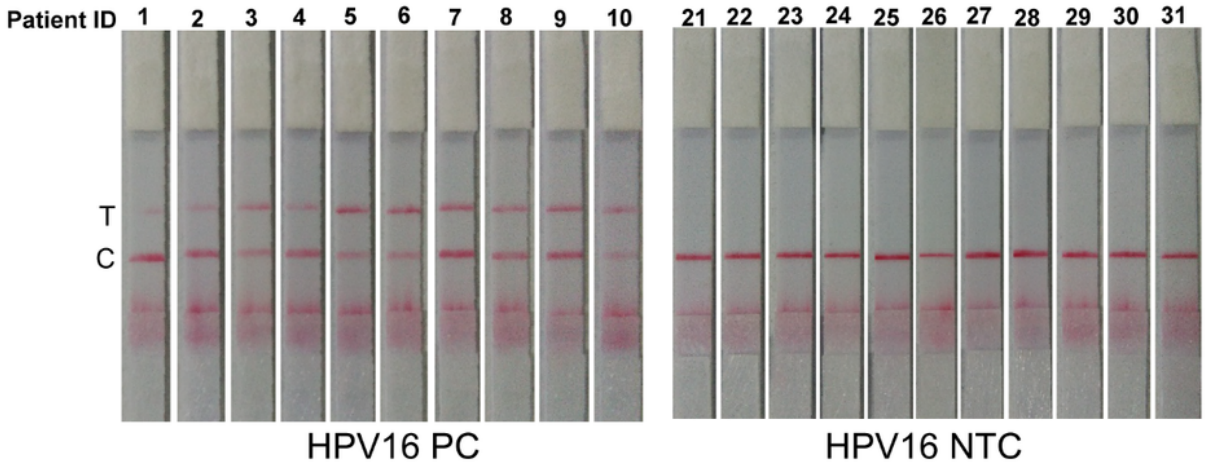

HPV16	qPCR positive	qPCR negative	Total number
TESTOR positive	10	0	21
CRISPR negative	0	11	

b

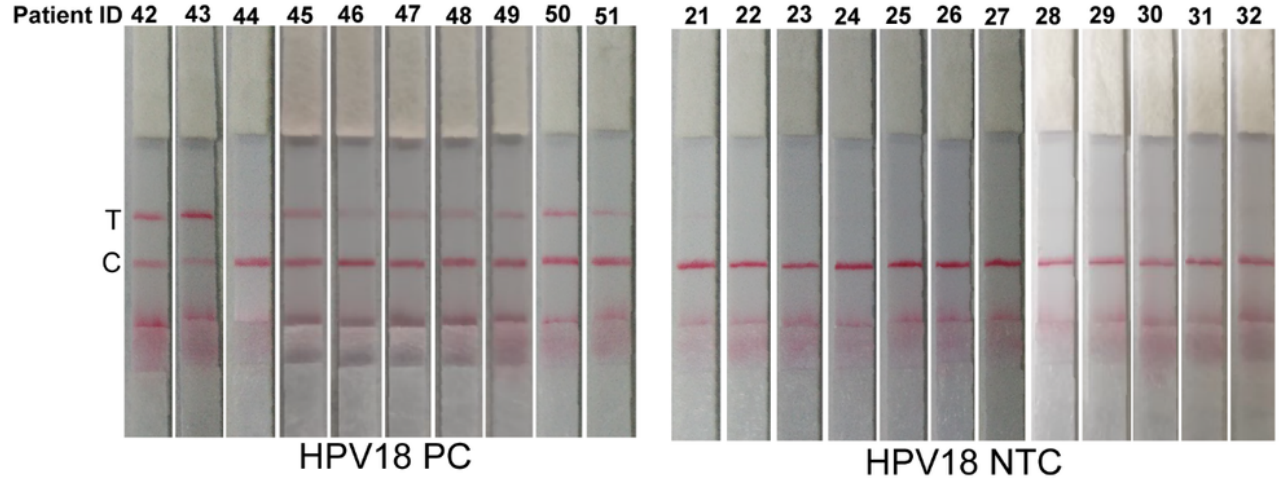

HPV18	qPCR positive	qPCR negative	Total number
TESTOR positive	10	0	22
TESTOR negative	0	12	

Figure 5

Detection of HPV in clinical samples using lateral flow TESTOR assay. a, Lateral flow strips showing HPV16 TESTOR assay results (upper panel). Ten qPCR-positive and eleven qPCR-negative samples were used for HPV16 detection. The Cas12a detection assays were run on lateral flow strips and imaged after 5 min. Performance characteristics of lateral flow TESTOR assay (bottom panel). A total of 21 clinical samples were evaluated using the lateral flow version of the TESTOR assay. Both the positive agreement and negative agreements are 100%. NTC, no-template control; T, test line; C, control line. b, Lateral flow strip readouts for HPV18 detection using clinical samples. A total of 21 clinical samples were evaluated (10 HPV18 positive and 12 negative). The onepot reactions were 1:10 diluted after incubation at 37oC for 30 min and then run on lateral flow strips and imaged after 5 min.

Supplementary Files

This is a list of supplementary files associated with this preprint. Click to download.

- Supplementaryfigures.docx